Acta Chemica Scandinavica, 1997: 51: 556–561
Printed in UK – all rights reserved

ACTA
CHEMICA SCANDINAVICA
ISSN 0904–213X

Electron Spin Relaxation and ESEEM Spectroscopy of the Glycine Radical in Diglycine Nitrate Single Crystal†

M. Gramza, W. Hilczer, J. Goslar and S. K. Hoffmann*

Institute of Molecular Physics, Polish Academy of Sciences, Smoluchowskiego 17, PL-60179 Poznań, Poland

Gramza, M., Hilczer, W., Goslar, J. and Hoffmann, S. K., 1997. Electron Spin Relaxation and ESEEM Spectroscopy of the Glycine Radical in Diglycine Nitrate Single Crystal. – Acta Chem. Scand. 51: 556–561. © Acta Chemica Scandinavica 1997.

Glycine radical NH_3^+–$\dot{C}$H–COO^- produced by X-ray irradiation was identified and characterized by cw-EPR and pulsed EPR methods. The isotropic hyperfine coupling are: $H_\alpha = 2.18$ mT, $H(NH_3) = 1.71$ mT and $^{14}N = 0.3$ mT at 295 K. The spin–lattice relaxation time was measured in the range 10–200 K by the saturation recovery method, and is described as the sum of the contributions from the direct process, distribution of the inter-radical couplings and the Murphy process with vibrational energy of 321 cm^{-1}. The phase memory time T_M was strongly temperature-dependent with two minima at 20 and 170 K related to the flipping motion of the glycine molecules and rotation of the NH_3 groups, respectively. The Fourier transform ESEEM spectrum consists of the proton matrix lines and very sharp lines in the nitrogen frequency region. They are interpreted as quadrupole frequencies under 'cancellation conditions' with quadrupole coupling constant 2.10 MHz, an asymmetry parameter of 0.7, and ^{14}N isotropic coupling $a_{iso} = 2.12$ MHz of the NH_3-group of the neighbouring glycine molecule.

Diglycine nitrate $(NH_2CH_2COOH)_2HNO_3$ (DGN) belongs to the glycine salt family exhibiting ferroelectric properties. An order–disorder type phase transition from the paraelectric (*Pa*) phase to the polar phase ($P2_1/a$) appears at $T_c = 206.5$ K.[1] The paraelectric phase of DGN is heavily disordered. It consists of distributed polar lattice cells (microdomains) of opposite polarity resulting from the two possible orientations of the polar glycine dimers coupled by a strong symmetric hydrogen bond. The nitrate anions NO_3^- occupy at random the four possible positions with different and temperature dependent occupancy.[2] The dynamic disorder and molecular motions determine most of the crystal properties in both paraelectric and ferroelectric phases.

An effective method for the study of local static and dynamic crystal properties is EPR spectroscopy. Since the DGN crystal lattice is not suitable for doping with 3d transition metal ions, a radical centre, produced by γ- or X-ray irradiation, must be used as the paramagnetic probe. Three types of free radical are formed in DGN. NO_3^- and $\dot{C}H_2COO^-$ radical are very unstable at room temperature[3–5] whereas the NH_3^+–$\dot{C}$H–COO^- zwitterionic radical is relatively stable and is discussed in this paper.

Various glycine-based free radicals induced by radiation of amino acids have been intensively studied by EPR and ENDOR techniques in different matrices,[6–9] and their electronic structure parameters and hyperfine coupling constants have also been calculated from *ab initio* quantum-mechanical calculations.[10,11] Over the past few years, scientific interest in glycine-centred radicals have been renewed in relation to the radical processes and radiation damage of protein molecules in biological materials.

New information about the radical dynamics and unpaired electron density distribution over the neighbouring molecules can be obtained by pulsed EPR spectroscopy. In this paper we present the electron spin–lattice and spin–spin phase relaxation as well as Fourier transform electron spin echo (ESE) spectra of NH_3^-–$\dot{C}$H–COO^- radical at various temperatures in DGN single crystal.

Results and discussion

Cw-EPR. Single crystal rotational data were collected in the three orthogonal planes of the crystallographic system *a*, *b*, *c**. The spectra are highly anisotropic and dominated by splittings from carbon α-proton and β-protons of the rotating NH_3 group with a further splitting into triplets from ^{14}N. An analysis of the splitting and diagonalization of the hyperfine and g^2-tensor gives the principal value of the anisotropic *A*-splittings collected in Table 1 and

* To whom correspondence should be addressed.

† Lecture held at the 14th International Conference on Radical Ions, Uppsala, Sweden, July 1–5, 1996.

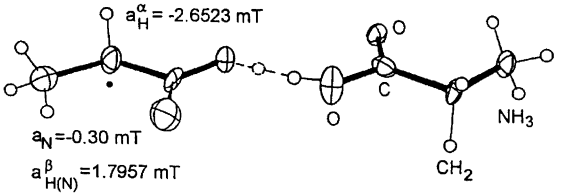

Fig. 1. Dimer of glycine molecules joined by a symmetrical hydrogen bond (two positions of the proton are marked) with radical ĊH on the left part of the dimer, and the isotropic hyperfine splitting from the α-proton, nitrogen and protons of a rapidly rotating NH_3-group, at room temperature.

g-factors $g_\parallel = 2.0053(5)$, $g_\perp = 2.0012(5)$. These data confirm that the paramagnetic centre is located on the carbon atom of the zwitter-ionic form NH_3^+–ĊH–COO^- of one part of the glycine dimer, as shown in Fig. 1 where the isotropic hyperfine splittings are also marked.

The data collected in Table 1 show that maximal hyperfine splitting of the α-proton is higher than reported previously,[4] although the a_{iso} values are very similar. Our isotropic hyperfine parameters are very close to those predicted by *ab initio* quantum-mechanical calculations for the zwitter-ionic form of the glycine radical in solution.[11]

Temperature dependence measurements showed that the EPR spectrum is not sensitive to the phase transition at $T_c = 206.5$ K and only a continuous line broadening is observed on cooling. This is due to a retardation of the NH_3-group's hindered rotation which becomes very slow on the EPR timescale at low temperatures allowing individual protons to give resolved lines in the EPR spectrum. On the basis of the temperature and rotational data we selected the *a*-axis direction for further pulsed EPR measurements since the lines from two magnetically inequivalent radical sites coincide and the EPR spectrum and FT-ESEEM spectrum are well split at this crystal orientation. The spectrum is presented in Fig. 2 together with the corresponding two-pulse ESE detected spectrum which is a relaxation-perturbed absorption EPR spectrum. Owing to the relaxation rate and weak intensity, the outer (low-field and high-field) hyperfine lines are

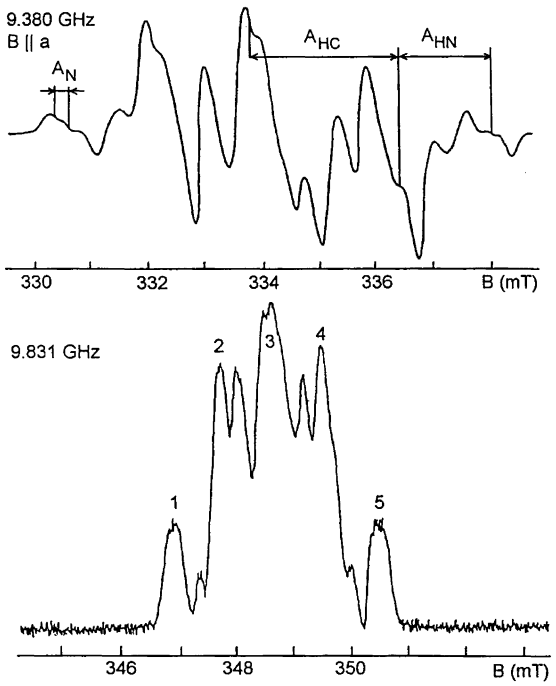

Fig. 2. Cw-EPR spectrum (9.380 GHz) and two-pulse field-swept echo detected spectrum recorded at room temperature along the *a*-axis. Because of the low intensity and short relaxation time the low field and high field hyperfine lines are not visible in the FS-ESE spectrum.

Table 1. Anisotropic *A* and isotropic a_{iso} hyperfine coupling constants (in mT)[a] for NH_3^+–ĊH–COO^- zwitter-ion radical in DGN, glycine and triglycine sulfate (TGS) crystals.

Crystal	$A_{H(C)}$	$A_{H(N)}$	A_N	Ref.
DGN	−3.570	1.960	–	
	−0.740	1.830	–	4
	−2.220	1.600	–	
	$a^\alpha_{iso} = -2.177$	$a^\beta_{iso} = 1.800$	–	
	−4.1219	2.4555		
	−0.9052	1.6178		This paper
	−2.9298	1.3137		
	$a^\alpha_{iso} = -2.6523$	$a^\beta_{iso} = 1.7957$	$a^N_{iso} = -0.3$	
α-Glycine	−3.451	1.9145	−0.3535	
	−1.365	1.6275	−0.3465	3
	−2.149	1.6100	−0.2465	
	$a^\alpha_{iso} = -2.321$	$a^\beta_{iso} = 1.7185$	$a^N_{iso} = -0.315$	
TGS	−3.2725	1.8795	−0.350	
	−1.9145	1.5505	−0.301	12
	−1.2705	1.4665	−0.252	
	$a^\alpha_{iso} = -2.1525$	$a^\beta_{iso} = 1.645$	$a^N_{iso} = -0.301$	
Theory[b]	$a^\alpha_{iso} = -2.68$	$a^\beta_{iso} = 1.89$	$a^N_{iso} = -0.35$	11

[a] A (MHz) = 28 A (mT). [b] For the zwitter-ionic radical in aqueous solution.

not detectable in the field-swept ESE spectrum and the pulsed experiments were performed for magnetic field settings marked as 1–5 on the spectrum.

Spin–lattice relaxation. The spin–lattice relaxation time T_1 was determined using a two-pulse ESE signal to monitor the magnetization recovery to an equilibrium after saturation. It was possible at low temperatures easily to saturate the separated EPR lines. This proves that the spectral diffusion is very slow or negligible in the crystal. Also, the effects of the spectral diffusion were not observed during spin–spin phase relaxation measurements as expected for a low concentration of the radical centres which is about 8×10^{17} spins/gram in our crystal. The recovery curve was non-exponential in the whole temperature range and was identical for the all five hf lines marked in Fig. 2. A non-exponential recovery is expected when spectral diffusion is competing with the spin–lattice relaxation processes, which seems not to be the case in the DGN crystal. The distribution of the relaxation times, phonon bottleneck, two different and independently relaxing centres and/or cross-relaxation can also lead to non-exponential recovery signals[13–15] which can be fitted to a sum of exponential functions (usually bi-exponential) or to the stretched exponentials in the case of the T_1 distribution. For radicals produced by X-irradiation in a crystal, a non-uniform distribution of radicals can be expected with different radiation damage around differently located radical centres implying different T_1-values. Indeed, for the glycine radical in DGN we were able to fit the experimental recovery curves by the stretched exponential given in eqn. (1), where V is a measure of the magnetization and β is a dispersion parameter. T_1 in eqn. (1) is an average value of the relaxation time distribution. The fitted T_1 values vs. temperature are shown in Fig. 3; with $\beta = 0.70(6)$ in the whole temperature range. The temperature variations of the relaxation rate can be fitted to eqn. (2).

$$V(t) = V_0\left[1 - \exp\left(-\frac{t}{T_1}\right)^{\beta}\right] \tag{1}$$

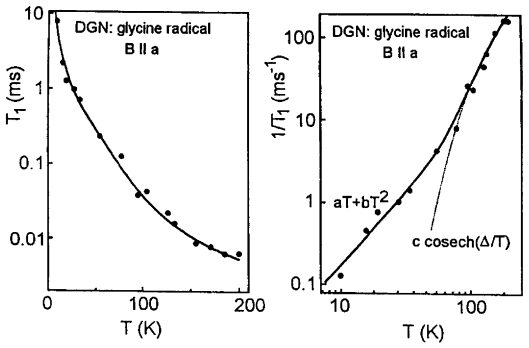

Fig. 3. Temperature dependence of the spin–lattice relaxation time T_1 and relaxation rate $1/T_1$. The solid lines are plots fitted to the equation $1/T_1 = aT + bT^2 + c\,\mathrm{cosech}(\Delta/T)$ with $\Delta = 462$ K (321 cm^{-1}) and *a*, *b*, *c* the parameters given in the text.

$$\frac{1}{T_1} = aT + bT^2 + c\,\mathrm{cosech}\left(\frac{\Delta}{T}\right). \tag{2}$$

The best fit is shown by the solid line in Fig. 3 with parameters: $a = 5\ K^{-1}\ s^{-1}$, $b = 1.2\ K^{-2}\ s^{-1}$, $c = 7 \times 10^5\ s^{-1}$, $\Delta = 462$ K (321 cm^{-1}). The linear term describes the contribution from the direct one-phonon relaxation process and is important at low temperatures. The quadratic term in the temperature dependence of the relaxation rate can be due to several mechanisms: spectral diffusion,[14] two-phonon Raman process above the Debye temperature,[16] a distribution of low-lying librational levels of the radical system,[14] and a distribution of the pairwise interactions between unpaired electrons in non-uniformly distributed radical systems.[14] The last two mechanisms have been observed and discussed in many organic radicals[14] and seem to operate in irradiated DGN crystals similarly to the glycine radical in triglycine sulfate (TGS) crystals.[17] The third term in eqn. (2) can be attributed to the local mode of the tunnelling rotation of the CH_3 or NH_3 group with tunnelling splitting $\Delta E = k\Delta/2$,[15] which is effective at low temperatures, or to the Murphy mechanism.[18] Murphy proposed an Orbach–Aminov type process whereby the absorption of a phonon causes simultaneous transition of a local vibration and the spin. Assuming this mechanism to be operative we have a low-lying librational excited state of energy $\Delta E = k\Delta = 321\ cm^{-1}$ for glycine radical in DGN. The same mechanism was identified for SeO_2^- radical in $KH_3(SeO_3)_2$ crystal with $\Delta = 52\ cm^{-1}$ and $123\ cm^{-1}$.[19]

Spin–spin phase relaxation. The phase memory time T_M in the crystal orientation studied varies from 0.30 μs to 5.8 μs depending on temperature as we reported previously.[20] The different hf lines relax with different T_M times (Fig. 4). Such behaviour is expected for anisotropic *g*-factors and hyperfine splitting when the phase relaxation is governed by time modulation of the *g* and *A* anisotropy. The two minima in the $T_M(T)$ dependence at about 20 K and 170 K are produced by two different molecular motions in the crystal. In the high-temperature minimum all lines are forced to relax with the same time T_M and the minimum is produced by a resonance-type shortening of T_M due to the hindered rotation of the NH_3-groups. The minimum appears on the transition from slow to fast rotation as compared with the splitting $\Delta\omega$ between unresolved spin packets formed by hf proton lines of the NH_3 groups of the glycine molecules surrounding the radical centre. For the slow rotation rate, i.e., when $\Delta\omega\tau_c > 1$, where τ_c is the NH_3 rotation correlation time, the electron spin echo decay can be described as $V = V_0 \exp(-2\tau/T_M)$ with $T_M = \tau_c$, whereas in the fast rotation limit, i.e., $\Delta\omega\tau_c < 1$ the kinetic equation has the same form but $T_M = 2/(\Delta\omega^2\tau_c)$.[21] Assuming an Arrhenius-type temperature dependence of the correlation time $\tau_c = \tau_0 \exp(E_a/RT)$ we are able to determine the motional parameters. The calculated $\tau_c(T)$ dependence around the minimum is presented as straight lines in the inset of Fig. 4 with parameters: $E_a = 12.0\ kJ\ mol^{-1}$, $\tau_0 =$

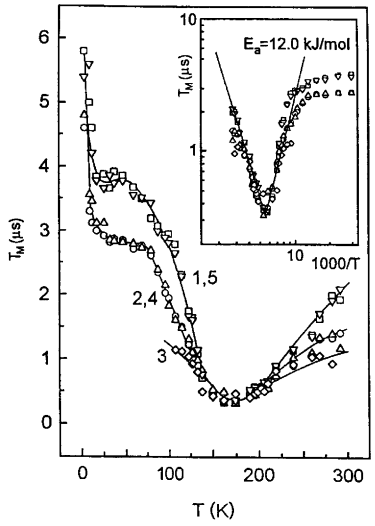

Fig. 4. Temperature dependence of the phase memory time T_M for the five hyperfine structure lines labelled as on the FS-ESE spectrum in Fig. 2. The inset shows log T_M vs. 10^3 K/T around the T_M minimum (170 K) with the result of fitting to the Arrhenius equation with $E_a = 12.0$ kJ mol^{-1} and $\tau_0 = 1.0 \times 10^{-9}$ s.

1.0×10^{-9} s and $\tau_c = 7 \times 10^{-5}$ s in the minimum. As can be seen from the inset, the symmetrical minimum characteristic for a thermally activated motion has the same activation energies for all hf lines. The E_a value is in the range of E_a determined from NMR relaxation studies in glycine salt crystals [$E_a = 29$ kJ mol^{-1} in α-glycine,[21] $E_a =$ 22.2 and 27.6 kJ mol^{-1} in TGS,[23] and $E_a = 10.7$ and 14.2 kJ mol^{-1} in triglycine fluoroberyllate (TGFB)].[24]

For the low-temperature minimum, a detailed analysis is impossible since the minimum is not well shaped, but it must be due to a relatively slow motion. We postulate that this is a flipping motion of the glycine molecule between two crystallographic positions[2] with a temperature-dependent flipping rate similar to the flipping type minimum we have observed for Cu^{II}-doped triglycine-selenate at about 50 K.

ESEEM. Modulated two-pulse electron spin echo decay was recorded and analysed for the five hf lines 1–5 of Fig. 2 at room temperature. The decay for line 1 presented in Fig. 5(a) demonstrates the existence of low (ν_N) and high frequency (ν_H) modulations characteristic for nitrogen and proton, respectively. A similar modulation pattern was observed for the other hyperfine components.

Fourier transform of the modulation function (pseudo-ENDOR or ESEEM spectrum) is shown in Fig. 5(b). The peaks ν_H and $2\nu_H$ at 14.8 MHz and 29.6 MHz are due to weakly coupled matrix protons from surrounding glycine molecules. In some crystal orientations, in addition to these peaks, doublets around ν_H are visible arising from strongly coupled protons.

The low frequency peaks are due to the dipolar coupling to the ^{14}N nuclei. This peak pattern is characteristic for the so-called *cancellation condition* when the nuclear nitrogen Zeeman interaction and isotropic hyper-

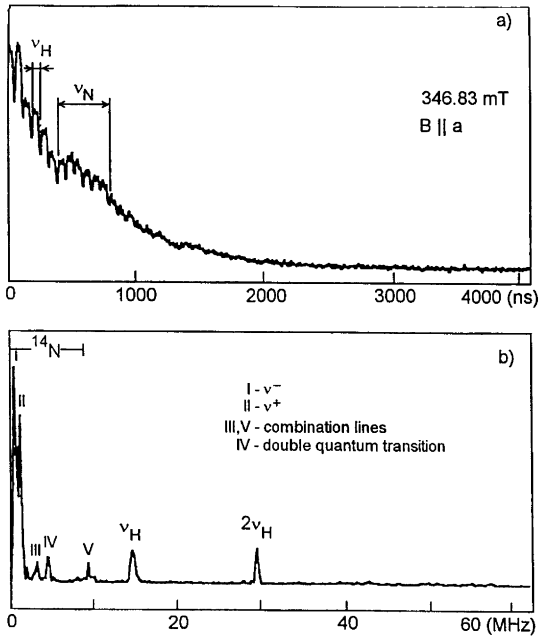

Fig. 5. (a) Two-pulse ESE decay at room temperature along the *a*-axis modulated with nuclear proton ν_H and nitrogen ν_N frequencies. (b) Fourier transform of the modulation function of the ESE envelope modulation (a). In addition to the proton peaks, five nitrogen peaks were observed and assigned.

fine coupling cancel each other,[25] i.e., when $\nu_N = a/2$ (a being the isotropic hyperfine constant). The peaks at 1.2 MHz and 1.98 MHz are the quadrupole ν^- and ν^+ frequencies, respectively. Peak IV at 4.53 MHz is the double quantum transition whereas the additional peaks III and V at 3.33 MHz and 9.38 MHz are the combination frequency due to interactions with more than one ^{14}N.

Owing to the anisotropy of hyperfine interaction, the observed modulation pattern is strongly orientation-dependent and a contribution to the modulations can be given only by the nuclei located at distances 0.3–0.5 nm from the unpaired electron. In this area lie the glycine molecules and NO_3^- groups as is shown in Fig. 6. When the magnetic field is directed along the *a*-axis, as in our experiment, one would expect the main contribution to the ESEEM pattern from protons and nitrogen from glycine GIII′ and nitrogen of the NO_3-groups. Under cancellation conditions one cannot expect the quadrupolar splitting from NO_3-groups since the dynamic four-positional disorder should average out the electric field gradient at the ^{14}N position. Thus observed ν^- and ν^+ frequencies are connected with the NH_3 group of glycine GIII′. The quadrupolar frequencies are given by eqn. (3),

$$\nu_0 = \frac{e^2qQ}{2h}\eta$$

$$\nu^- = \frac{e^2qQ}{4h}(3-\eta) \qquad (3)$$

$$\nu^+ = \frac{e^2qQ}{4h}(3+\eta)$$

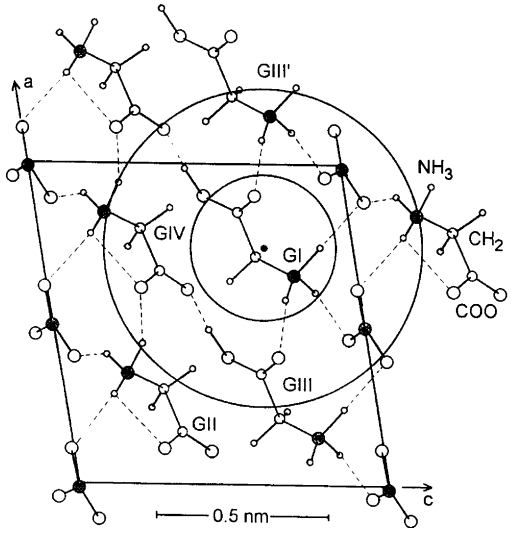

Fig. 6. Distribution of the glycine and nitrate groups in the *ac*-plane around glycine GI with a radical centre. Magnetic nuclei located in the area between two circles (with radii 0.3 and 0.5 nm) are expected to contribute to the ESEEM. For $B_{\|}a$ the main contribution is given by NH_3-group of the glycine GIII'.

where e^2qQ/h is the quadrupolar coupling constant and $\eta=(V_{xx}-V_{yy})/V_{zz}$ is an asymmetry parameter with V_{ij} being the electric field gradient tensor component. The ν_0 frequency is too low to be resolved in the FT-spectrum of Fig. 5, and observed ν^- and ν^+ values lead to $e^2qQ/k=$ 2.10 MHz and $\eta=0.7$. The quadrupolar coupling constant has a value typical of amine groups of amino acids.[26]

The double quantum transition ($\Delta M_I=2$) appears at the frequency given in eqn. (4), where ν_N is the nitrogen Zeeman frequency ($\nu_N=1.06$ MHz at $B=346.83$ mT). Taking e^2Qq and η calculated above we obtain the value of the isotropic hyperfine coupling $a=2.12$ MHz, which is a measure of the unpaired electron density on the ^{14}N nuclei of the glycine GIII' at a distance of 0.465 nm from the radical centre. This is a unique parameter which cannot be determined by cw-EPR spectroscopy.

$$\nu_{dq}^{\pm}=2\left[\left(\nu_N\pm\frac{a}{2}\right)^2+\left(\frac{e^2qQ}{4h}\right)^2(3+\eta)^2\right]^{1/2} \qquad (4)$$

Experimental

DGN crystals were obtained by slow evaporation of an aqueous stoichiometric solution of glycine and nitric acid at room temperature. The crystals were irradiated with X-rays for 1 h at room temperature by W Kα radiation (45 kV, 20 mA). After such irradiation radicals of concentration (of about 8×10^{17} spins g^{-1}) suitable for EPR and ESE measurements were obtained.

Continuous wave and pulsed EPR measurements were made on a Bruker ESP380 FT/CW spectrometer operating with a dielectric resonator equipped with an Oxford Instruments CF935 liquid helium cryostat.

The spin–lattice relaxation time T_1 was measured by the saturation recovery method with a sequence of eight 24 ns saturation pulses and two 48 ns reading pulses generating a Hahn echo signal. The recovery of the magnetization to the equilibrium state was non-exponential as discussed in the text.

The phase memory time and ESEEM were studied using the two-pulse technique. Two 48 ns microwave pulses were used with the amplitude adjusted to obtain maximum ESE intensity. The initial separation of pulses was set to 200 ns and then increased by 8 ns steps. The pulse sequence repetition time was set to $5T_1$. The observed ESE decay curves were fitted to the monoexponential function $V=V_0\exp(-t/T_M)$ and the modulations were subtracted from the decay using the internal spectrometer routine.

Acknowledgements. This work was supported by Research Project KBN-2-P03B-038–08 of the Polish Scientific Research Committee.

References

1. Sato, A. *J. Phys. Soc. Jpn. 25* (1968) 185.
2. Łukaszewicz, K., Pietraszko, A. and Stępień-Damm, J. *Polish J. Chem. 70* (1996) 1550.
3. Collins, M. A. and Whiffen D. H. *Mol. Phys. 10* (1966) 317.
4. Ohashi, S., Abe, R. and Kawamura, A. *J. Phys. Soc. Jpn. 34* (1973) 1694.
5. Dikanov, S. A. and Astashkin, A. V. In: Hoff, A. J., Ed., *Advanced EPR Applications in Biology and Biochemistry*, Elsevier, Amsterdam 1989, Chap. 2.
6. Kato, T. and Abe, R. *J. Phys. Soc. Jpn. 3* (1972) 717.
7. Nunome, K., Muto, H., Toriyama, K. and Iwasaki, M. *J. Chem. Phys. 65* (1976) 3805.
8. Goslar, J., Piekara-Sady, L. and Kispert, L. D. In: Poole, Ch. P. Jr. and Farach, H. A., Eds., *Handbook of Electron Spin Resonance*, AIP Press, New York 1994, Chap. VI.
9. Kotake, Y. and Miyagawa, I. *J. Chem. Phys. 64* (1976) 3169.
10. Barone, V., Adamo, C., Grand, A., Jolibois, F., Brunel, Y. and Subra, R. *J. Am. Chem. Soc. 117* (1995) 12618.
11. Barone, V., Adamo, C., Grand, A. and Subra, R. *Chem. Phys. Lett. 242* (1995) 351.
12. Dezor, A. Ph.D. Thesis, Institute of Molecular Physics, Polish Academy of Sciences, Poznań 1969.
13. Steven, S. B. and Stapleton, H. J. *Phys. Rev. B 42* (1990) 9794.
14. Dalton, L. R., Kwiran, A. L. and Cowen, J. A. *Chem. Phys. Lett. 17* (1972) 495.
15. Bowman, M. K. and Kevan, L. In: Kevan, L. and Schwartz, R. N., Eds., *Time Domain Electron Spin Resonance*, Wiley, New York 1979, Chap. 3.
16. Hoffmann, S. K., Hilczer, W. and Goslar, J. *J. Magn. Reson. A 122* (1996) 37.
17. Voelkel, G., Brunner, W., Windsch, W. and Steudel, D. *Phys. Stat. Sol. (b) 95* (1979) 99.
18. Murphy, J. *Phys. Rev. 145* (1966) 241.
19. Ivanshin, V. A., Kurkin, I. N., Brunner, W. and Voelkel, G. *Phys. Stat. Sol. (b) 151* (1989) K53.
20. Hoffmann, S. K., Gramza, M. and Hilczer, W. *Ferroelectrics 172* (1995) 431.
21. Tsvetkov, Yu. D. and Dzuba, S. A. *Appl. Magn. Reson. 1* (1990) 179.

22. Andrew, E. R., Hinshaw, W. S. and Hutchins, M. G. *J. Magn. Reson. 15* (1974) 196.
23. Ślóasarek, G., Idziak, S., Piślewski, N. and Stankowski, J. *Phys. Stat. Sol. (b) 110* (1982) 233.
24. Piślewski, N. and Grosescu, R. *Bull. Acad. Sci. XX* (1972) 1027.
25. Peisach, J. In: Karlin, K. D. and Tyeklár, Z., Eds., *Bioinorganic Chemistry of Copper*, Chapman and Hall, New York 1993, p. 21.
26. Rabbani, S. R., Edmonds, D. T., Gosling, P. and Palmer, M. H. *J. Magn. Reson. 72* (1987) 230.

Received July 1, 1996.